RSC Sustainability

ROYAL SOCIETY OF CHEMISTRY

PAPER

View Article Online
View Journal | View Issue

Cite this: *RSC Sustainability*, 2026, **4**, 987

Integrated multi-stream valorization of kitchen food waste through enzymatic hydrolysis and selective fermentation

Shubhangi Arvelli,[a] Deokyeol Jeong,[bc] Mairui Zhang,[a] Linjing Jia,[a] Haixin Peng,[a] Ji Qi,[a] Nilofar Arabi,[a] Seyedamirreza Babaei,[a] Eun Joong Oh[bc] and Jikai Zhao *[a]

Received 2nd October 2025
Accepted 7th January 2026

DOI: 10.1039/d5su00778j

rsc.li/rscsus

Food waste (FW) management has emerged as a global priority due to its environmental burden and loss of valuable resources. Kitchen FW, rich in carbohydrates, proteins, and fats, has a great potential for the bioconversion of value-added products. Conventional valorization strategies have largely focused on single-product pathways. This study explored a component-specific conversion strategy to recover fats, hydrolyze starch, ferment glucose to ethanol and 3-hydroxypropionic acid (3-HP), and obtain proteins from kitchen FW. Results showed that 62.64% of fats were first separated from kitchen FW, and they were rich in oleic acid (C18 : 1, 34.14%), linoleic acid (C18 : 2, 24.64%), palmitic acid (C16 : 0, 20.14%), and stearic acid (18 : 0, 6.81%). The hydrolysis time, enzyme dosage, and temperature were optimized using a one-step enzymatic hydrolysis (OSEH) of starch, employing response surface methodology. This optimization resulted in a starch hydrolysis efficiency of 82% and a glucose concentration of 60 g L^{-1}. Using the resulting glucose hydrolysate, 21 g L^{-1} of ethanol (0.35 g g^{-1} glucose) and 12 g L^{-1} of 3-HP (0.20 g g^{-1} glucose) were produced with *Saccharomyces cerevisiae* and *Issatchenkia orientalis*, respectively. The protein-rich (>68%) residue after OSEH contained about 50% of glutamic acid, aspartic acid, leucine, valine, and alanine. This work provides new insights into multi-product biorefineries for precision FW valorization, enabling waste reduction and advancing a circular bioeconomy.

Sustainability spotlight

Food waste is often underutilized and largely destined for landfills, contributing to environmental and social burdens. This study presents a sustainable multi-stream valorization pathway that efficiently recovers fats, proteins, and starch. The outcomes directly contribute to the United Nations Sustainable Development Goals, particularly SDG 7 (Affordable and Clean Energy), SDG 12 (Responsible Consumption and Production), and SDG 13 (Climate Action). Through waste-to-resource integration, this work demonstrates practical and scalable solutions that advance global sustainability objectives.

1. Introduction

Food waste (FW) is a critical global issue with profound environmental, social, and economic implications. More than 1.3 billion tonnes of food are wasted annually, representing a major loss of edible resources and natural inputs such as land, water, and energy used in food production.[1] Conventional disposal methods, including landfilling, composting, and incineration, might aggravate this issue by squandering valuable nutrients while contributing significantly to greenhouse gas emissions, soil contamination, and other environmental burdens.[2] Given its rich composition of carbohydrates, proteins, fats, and micronutrients, FW is a promising feedstock for bioconversion into value-added products.[3] However, traditional valorization efforts have largely focused on single-product pathways such as anaerobic digestion for biogas generation, which underutilize the full potential of FW and offer limited environmental benefits.[4] Recent advances in bioprocessing and precision fermentation highlight opportunities to recover higher-value products, including bioplastics, enzymes, organic acids, and bio-adsorbents, while maintaining lower energy demand and a reduced environmental footprint.[5–8] Such strategies align with the principles of the circular economy, the United Nations Sustainable Development Goals (Agenda 2030), and biorefinery concepts (IEA Task 42), which emphasize prioritizing the production of high-value chemicals over bioenergy.[9,10]

FW typically comprises a diverse mix of starch, fats, proteins, water, and minerals. This variability necessitates physicochemical pretreatment to enhance downstream processing.[11] Pretreatment can reduce the moisture content, improve

[a]*Carl and Melinda Helwig Department of Biological and Agricultural Engineering, Kansas State University, Manhattan, KS 66506, USA. E-mail: jikaizhao@ksu.edu*
[b]*Whistler Center for Carbohydrate Research, Purdue University, West Lafayette, IN 47907, USA*
[c]*Department of Food Science, Purdue University, West Lafayette, IN 47907, USA*

homogeneity, and increase the accessibility of fermentable sugars, thereby facilitating microbial growth and metabolite accumulation.[12] While free monosaccharides such as glucose can be directly consumed, complex carbohydrates require hydrolysis. Acid hydrolysis is efficient in releasing sugars but often generates inhibitory compounds, such as furans. In contrast, enzymatic hydrolysis is more selective, operates under milder conditions, reduces inhibitor formation, and minimizes equipment corrosion.[13–15] Nevertheless, the high cost of commercial enzymes remains a bottleneck, underscoring the importance of optimizing hydrolysis to reduce enzyme loading, reaction time, and energy consumption.[16] Approaches such as in-house enzyme production, enzyme cocktails, simultaneous saccharification and fermentation, and microwave- or ultrasound-assisted hydrolysis have been explored to improve enzymatic efficiency.[17–20] Fermentable sugars obtained from the enzymatic hydrolysis of FW starch represent a versatile platform for bioconversion into value-added chemicals. While ethanol remains the most widely produced bioproduct from FW sugars, interest has recently shifted toward higher-value chemicals. Among these, 3-hydroxypropionic acid (3-HP) has been identified by the U.S. Department of Energy as one of the top 12 platform chemicals due to its role as a precursor for bioplastics, acrylics, and other industrial applications.[21] This highlights the potential of FW starch as a substrate not only for conventional bioethanol production but also for next-generation biochemicals. Although 3-HP has been produced from defined substrates such as sugarcane juice, molasses, and lignocellulosic biomass, using different microorganisms.[22–24] However, its production from real kitchen FW remains underexplored due to substrate heterogeneity, variable nutrient composition, and the presence of fermentation inhibitors.

The fat fraction, largely derived from meat, fish, dairy, and oily sauces, constitutes a major component of FW.[25] Its fatty acid (FA) chain length and saturation profile are crucial in selecting suitable valorization pathways.[12] For instance, fat fractions may serve as biodiesel precursors,[17,18] production of biolubricants,[26] bisabolene,[27] liquid detergents,[28] plasticisers,[29,30] polyurethane foams[31,32] and surfactants,[33] underscoring its versatility as a sustainable raw material. Proteins recovered from FW also hold promise for applications in the nutraceutical, pharmaceutical, cosmetic, and animal feed industries. Hydrolyzed protein fractions are particularly valuable, as they contain essential amino acids and bioactive peptides that support both feed applications and microbial cultivation.[34] Mineral fractions (*e.g.*, Na, K, Ca, Mg, with trace elements such as Zn, Mn, Fe, and Cu) add further value, as certain elements can facilitate microbial biodiesel production (*e.g.*, by microalgae).[35,36]

Although FW valorization has been extensively investigated, most studies focus on single-product recovery or isolated processing streams. In contrast, limited attention has been given to the systematic valorization of kitchen FW through integrated multi-stream pathways. The novelty of this work lies in the sequential and comprehensive utilization of all major fractions of kitchen FW within a single framework. Specifically, fats were first selectively removed and characterized, followed by enzymatic conversion of the starch-rich slurry using both one-step (OSEH, namely, simultaneous liquefication and saccharification) and two-step (TSEH, namely, separate liquefication and saccharification) hydrolysis strategies. The resulting glucose hydrolysate was subsequently converted into either ethanol or 3-hydroxypropionic acid using separate microorganisms. In addition, FA composition of the recovered fats and amino acid profiles of the protein residues were measured to assess their potential for downstream applications. This integrated approach moves beyond conventional single-stream valorization by enabling alternative and sequential utilization of major kitchen FW fractions, thereby provides a practical biorefinery strategy for generating multiple high-value products.

2. Materials and methods

2.1 Feedstock preparation

The FW utilized in this study was sourced from the Kramer Dining Canter at Kansas State University, located in Manhattan, Kansas. The waste stream primarily consisted of leftover and post-consumed food items such as pizza, pasta, bread, fruits, vegetables, water, cheese, and meat. The non-food materials, such as napkins, plastic, and bones, were separated. Upon collection, the FW exhibited an average moisture content of 77%. To ensure consistency and uniformity, the FW was ground using a food processor to reduce particle size and achieve homogenization. The resulting FW samples were then portioned into ziplock bags and stored at −20 °C until further analysis. Table 1 shows the initial composition of raw FW (R-FW) and defatted FW (D-FW).

2.2 Fat separation

The homogenised FW was thawed under refrigerated conditions (4 °C). Before enzymatic hydrolysis, fats were separated from FW to reduce interference during hydrolysis and to enable independent characterisation of the recovered FW fats (FWFs). The R-FW slurry was equilibrated to room temperature (24 ± 1 °C) and centrifuged at 10 000 × *g* for 15 min. A distinct FWF layer at the top was carefully aspirated using a sterile transfer pipette and collected in clean, labelled glass vials. The recovered FWFs were stored at −20 °C for subsequent analysis of their FA profile.

2.3 Enzymatic hydrolysis

The D-FW residue was subjected to enzymatic hydrolysis using two distinct strategies. TSEH was carried out using α-amylase

Table 1 Composition of raw and defatted FW on a dry basis

Component	R-FW (%)	D-FW (%)
Crude protein	23.78	28.75
Crude fat	44.23	16.52
Crude fiber	2.69	2.67
Ash	5.67	8.49
Starch	23.65	43.55

Table 2 Independent variables and their coded and actual levels for optimizing OSEH of FW starch

			Coded level of variable		
Factor	Factor code	Units	−1	0	1
Time	A	h	6	15	24
Enzyme	B	%	1	3	5
Temperature	C	°C	30	45	60

(Liquozyme® SC DS) and glucoamylase (Spirizyme® Ultra), with slight modifications.[37] The D-FW samples were adjusted to pH 5.5 and first treated with Liquozyme (0.025% of total solids) for liquefaction at 50 °C for 16 h, followed by Spirizyme (0.025% of total solids) for saccharification at 60 °C for 8 h.

OSEH was performed using Stargen™ 002, a commercial blend containing both α-amylase and glucoamylase, which enables OSEH, thereby reducing processing time and operational complexity without compromising starch hydrolysis efficiency. The parameters selected for optimization such as hydrolysis time (6–24 h), enzyme concentration (1–5% w/w of total solids), and temperature (30–60 °C), were chosen based on their influence on starch depolymerization efficiency and enzymatic activity, as reported in prior food-waste and starch-hydrolysis studies, as well as preliminary screening experiments (Table 2).[11] Hydrolysis time was selected to capture both rapid and extended conversion regimes while maintaining industrial feasibility. Enzyme concentration was varied to evaluate the trade-off between hydrolysis efficiency and enzyme cost, a key consideration for process scalability. Temperature was selected within the recommended operational range of Stargen™ 002 to ensure enzyme stability while assessing its effect on reaction kinetics. The parameter ranges were further constrained by the physicochemical characteristics of kitchen FW and practical considerations related to energy consumption and process integration. Optimization was conducted using response surface methodology with a central composite design implemented in JMP® Student Edition 18. Nineteen experimental runs, comprising 8 factorial points, 6 axial points, and 5 center points, were performed to investigate the linear, quadratic, and interaction effects of the selected factors (Table 3). The response variable was starch hydrolysis efficiency, as the experimental data were fitted to the following second-order polynomial.

$$Y = \beta_0 + \beta_1 A + \beta_2 B + \beta_3 C + \beta_{12} AB + \beta_{13} AC + \beta_{23} BC + \beta_{11} A^2 + \beta_{22} B^2 + \beta_{33} C^2$$

where Y represents starch hydrolysis efficiency; A, B, and C represent hydrolysis time, enzyme concentration, and temperature, respectively. Model adequacy and statistical significance were evaluated using one-way analysis of variance (ANOVA), and the optimum conditions were identified using the desirability function in JMP. Following hydrolysis under both strategies, the enzymes were inactivated by heating the FW slurry to 85 °C for 10 min. The hydrolysates were centrifuged at 770 × g for 30 min at 4 °C. The resulting supernatants were filtered, while the solid fractions were lyophilized and stored at −20 °C for further analysis.

2.4 Ethanol fermentation

The yeast broth containing glucose (20 g L^{-1}), peptone (5 g L^{-1}), yeast extract (3 g L^{-1}), KH_2PO_4 (1 g L^{-1}), and $MgSO_4 \cdot 7H_2O$ (0.5 g L^{-1}) was mixed thoroughly and sterilized in an autoclave at 121 °C for 20 min. For yeast activation, 1 g of *S. cerevisiae* (Red Star Ethanol Red, Lesaffre, USA) was suspended in 19 mL of sterile broth and incubated at 38 °C for 20 min, resulting in

Table 3 The OSEH starch hydrolysis efficiency under different conditions

Run	Pattern	Time (h)	Enzyme (%)	Temperature (°C)	Hydrolysis efficiency (%)
1	00A	15	3	60	68.36
2	+−+	24	1	60	56.62
3	−+−	6	5	30	50.93
4	000	15	3	45	63.13
5	000	15	3	45	65.92
6	0a0	15	1	45	48.37
7	++−	24	5	30	76.15
8	+++	24	5	60	82.80
9	+−−	24	1	30	46.24
10	a00	6	3	45	52.75
11	−++	6	5	60	60.84
12	0A0	15	5	45	73.79
13	A00	24	3	45	63.95
14	—	6	1	30	36.66
15	000	15	3	45	63.77
16	000	15	3	45	66.60
17	−−+	6	1	60	41.76
18	00a	15	3	30	53.80
19	000	15	3	45	65.94

a cell density of approximately 1×10^9 cells per mL.[38] Fermentation was initiated by inoculating 30 mL of hydrolysate (from TSEH or OSEH) with 1 mL of the activated yeast culture in a sterile Erlenmeyer flask. The flasks were fitted with airlocks to maintain anaerobic conditions at 32 °C with shaking at 150 rpm for 72 h in a rotary shaker (Model I2400, New Brunswick Scientific, USA).

2.5 3-Hydroxypropionic acid fermentation

3-HP fermentation was carried out using the engineered *I. orientalis* strain IoDY01H that has a heterologous oxidoreductase xylose and β-alanine-based 3-HP pathway. Pre-cultures were initiated by inoculating cells into 10 mL of YPD broth (20 g L^{-1} glucose, 20 g L^{-1} peptone, 10 g L^{-1} yeast extract) and incubating at 30 °C with agitation at 250 rpm for 24 h. After cultivation, cells were harvested by centrifugation, washed, and resuspended in sterile distilled water to an OD600 of 1.0.[39] Fermentation was conducted in 50 mL Erlenmeyer flasks containing 10 mL of hydrolysate (from TSEH or OSEH) with an adjusted pH of 4.2–4.8. Each flask was inoculated with the cell suspension and incubated at 30 °C with shaking at 250 rpm.

2.6 Analytical methods

2.6.1 Food waste composition analysis. The composition of FW at each processing step was analyzed by the University of Missouri Agricultural Experiment Station Chemical Laboratories. Moisture content was determined using the vacuum oven method (AOAC Official Method 934.01, 2006). Crude protein content was measured by combustion analysis using a LECO system following AOAC Official Method 990.03 (2006). Fat content was assessed *via* ether extraction in accordance with AOAC Official Method 920.39(A). Ash content was determined using AOCS Official Method Ba 5b-68, and crude fiber was analysed according to AOAC Official Method 978.10 (2006). Total starch content was calculated by difference using the formula: 100-(% protein, % fat, % moisture, % ash, % fiber). A complete amino acid profile was determined using the AOAC Official Method 982.30 E (a–c), Chapter 45.3.05 (2006). FAs were analyzed in the form of methyl esters using gas–liquid chromatography (GLC) following AOAC Official Method 996.06. Methyl esters were prepared using AOAC Method 965.49 and AOCS Official Method Ce 2–66.

2.6.2 Sugar and product quantification. Glucose, acetate, 3-HP, and ethanol concentrations in the liquor were measured using the same methods as described previously.[39,40] Glucose and ethanol concentrations of the hydrolysate and fermentation slurry were quantified using an Agilent 1260 Infinity HPLC system (Agilent Technologies, Santa Clara, CA, USA).[40] An HPX-87H organic acid column (7.8 mm × 300 mm, Bio-Rad Laboratories, Hercules, CA) or a Rezex-ROA organic acid column (150 mm × 4.6 mm; Phenomenex Inc., Torrance, CA, USA) maintained at 60 °C was used with a refractive index detector setting at 45 °C. For 3-HP quantification, the column temperature was maintained at 14 °C. The mobile phase was 5 mM H_2SO_4 at a flow rate of 0.6 mL min^{-1}.

2.7 Statistical analysis

All data were analysed using ANOVA, and significant differences among means were determined by Tukey's Honest Significant Difference (HSD) test at a significance level of $\alpha = 0.05$. Statistical analysis was performed using SPSS software (Version 19.0, SPSS Inc., Chicago, IL, USA). All treatments were conducted in duplicate unless otherwise specified.

3. Results and discussion

3.1 Removal of fats and analysis of fatty acid profiles

High fat content in FW reduces the carbon-to-nitrogen ratio and promotes acidification during anaerobic digestion,[41] while excess fats hinder oxygen transfer and lower process efficiency.[42] Liposoluble constituents in oils have been shown to modulate enzymatic activity,[43] and major FAs such as oleic, linoleic, and palmitic acids can inhibit α-amylase and α-glucosidase.[44] Upon hydrolysis, fats release long-chain FAs that adsorb to microbial cell surfaces,[45] impairing activity and destabilizing the process. These inhibitory effects underscore the importance of fat removal as a critical first step in FW valorization. The mechanical defatting process significantly reduced the fat content from 44.23% in R-FW to 16.52% in D-FW, corresponding to a fat removal of 27.71 g/100 g dry matter and a fat reduction efficiency of 62.63% (Table 1). This removal resulted in a proportional enrichment of crude protein from 23.78% to 28.75% and a rise in starch content from 23.65% to 43.55%. The simplicity of mechanical defatting, compared to solvent-based extraction methods, further highlights its suitability for sustainable bioprocessing as it does not chemically alter the remaining constituents and requires no additional reagents.[46,47]

The recovered FWFs exhibited a diverse FA profile dominated by oleic acid (C18 : 1, 34.1%), linoleic acid (C18 : 2, 24.6%), palmitic acid (C16 : 0, 20.1%), and stearic acid (C18 : 0, 6.8%) (Fig. 1). Minor fractions included linolenic acid (C18:3n3,

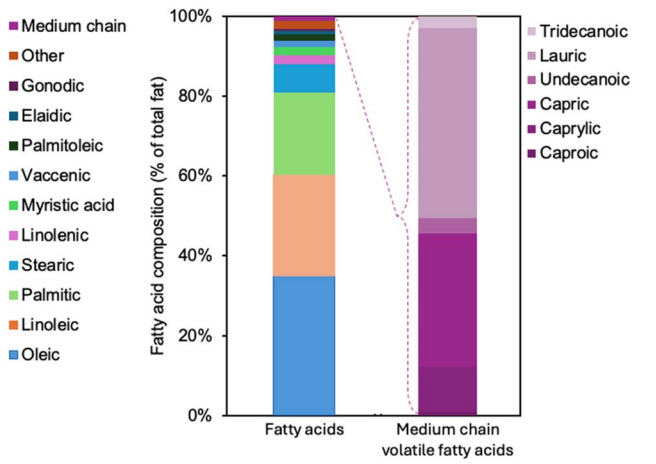

Fig. 1 Relative distribution of long-chain FAs and composition of medium-chain FAs of FWFs expressed as percentage of total fat and percentage of total medium-chain fatty acids.

2.2%), palmitoleic acid (C16 : 1, 1.4%), and vaccenic acid (C18 : 1 *cis*-11, 1.6%), with trans fatty acids such as elaidic acid (C18 : 1 *trans*-9) detected at 0.9%. Long-chain monounsaturated gondoic acid (C20:1n9) accounted for 0.6%. Medium-chain FAs contributed less than 1% of the total FAs, represented mainly by lauric (C12 : 0, 0.5%) and capric acid (C10 : 0, 0.4%), along with trace amounts of caproic (C6:0, 0.01%), caprylic (C8:0, 0.1%), undecanoic (C11 : 0), and tridecanoic acid (C13 : 0).

It was found that the physicochemical properties of the biodiesel are strongly dependent on the FA profile. The major FAs in FWFs, including oleic, palmitic, and linoleic acids, fall within the typical range reported for various vegetable oils (oleic acid: 6.2–71.1%, palmitic acid: 4.6–20.0%, linoleic acid: 1.6–79%).[48,49] Unique FA methyl esters with average carbon chain length 14.6 are associated with lower distillation temperatures (T90) and higher cetane numbers compared to soybean biodiesel.[50] The high content of unsaturated FAs (oleic and linoleic) contributes to favourable cold flow properties but may lead to increased NO_x emissions and reduced oxidative stability in biodiesel.[51] Conversely, saturated FAs, particularly long-chain types such as palmitic and stearic acids, provide enhanced oxidative stability and lower NO_x emissions, albeit with poorer cold flow properties. Oleic acid, which is abundant in FWFs and in most biodiesel feedstocks, exhibits a balance of these properties, combining the oxidative stability of saturated FAs with the favourable cold flow of unsaturated FAs.[51] The balanced composition of saturated and unsaturated FAs in FWFs indicates its suitability as a feedstock for biodiesel production. In this study, biodiesel production was not conducted, as it is a well-established process. However, future work could focus on demonstrating biodiesel quality following further purification of the FAFs.

3.2 Enzymatic hydrolysis of starch to boost glucose concentration

Conventional TSEH achieved a starch hydrolysis efficiency of 81.6% but required sequential enzyme addition and longer processing times. With reduced time and handling, the optimized OSEH process might achieve comparable efficiency, as confirmed by a highly significant quadratic model ($p < 0.0001$, $R^2 = 0.9964$). The model showed excellent fit, with a coefficient of variation (CV) < 10% and no significant lack of fit ($F = 5.47$, $p = 0.06$).[52] Factor ranking based on the F-value indicated enzyme dose (B) as the most significant variable, followed by time (A) and temperature (C). Among the quadratic terms, only A^2 was significant ($p = 0.03$), indicating a nonlinear effect, while B^2 and C^2 were not significant. The fitted quadratic regression equation for starch hydrolysis efficiency (Y) is expressed below.

$$Y = -3.623 + 2.008A + 5.745B + 0.955C + 0.158AB + 0.001AC + 0.004BC - 0.054A^2 - 0.428B^2 - 0.007C^2$$

Three-dimensional surface plots illustrated the effects of independent variables on hydrolysis efficiency (Fig. 2). For interaction terms, the combined effect of $A \times B$ was significant ($p < 0.05$) (Table 4), consistent with the 3D surface (Fig. 2a). Hydrolysis efficiency increased with longer reaction time, higher enzyme concentrations, and elevated temperatures. Hydrolysis efficiency increased markedly with higher enzyme concentrations and optimal reaction times (Fig. 2a). This aligns with previous studies showing that extended processing time allows enzymes greater opportunity to bind and hydrolyse substrates.[53] Hydrolysis efficiency was attributed to the breakdown of α-(1–4) glycosidic bonds in starch granules and further

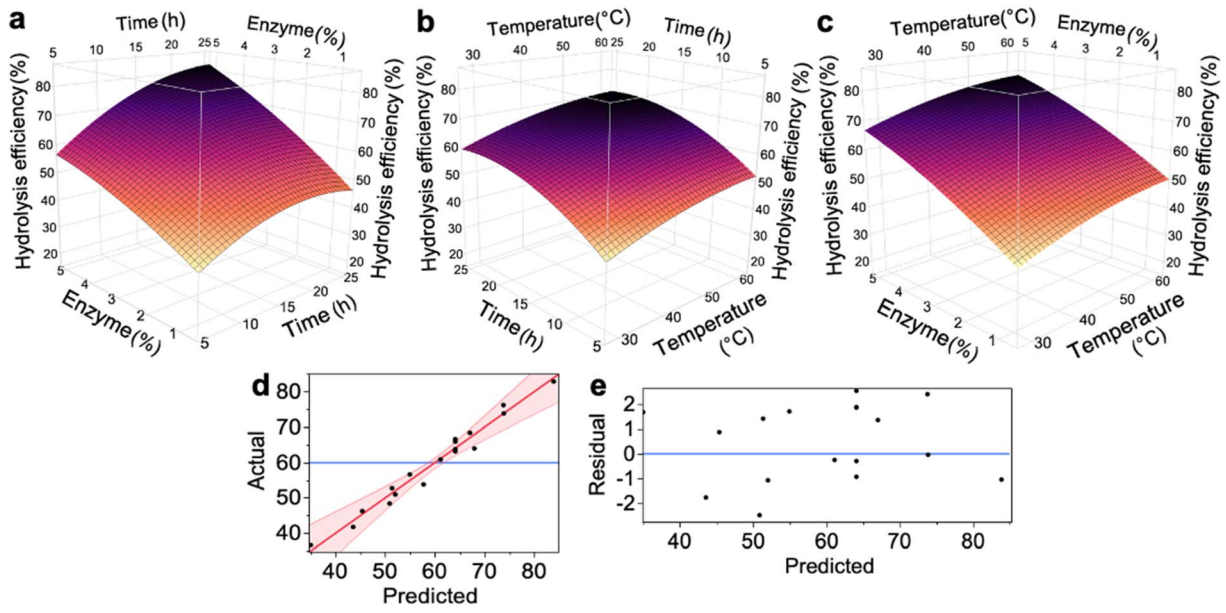

Fig. 2 3-D RSM illustration of changes in starch hydrolysis efficiency. (a) The interaction effect of time and enzyme dose; (b) temperature and enzyme dose; (c) temperature and time; (d) evaluation of model performance in validating optimization process for starch hydrolysis efficiency through actual *vs.* predicted values; (e) residual *vs.* predicted plots for starch hydrolysis efficiency.

Table 4 Analysis of variance for the quadratic model of OSEH starch hydrolysis efficiency

Source	DF	Sum of square	Mean sum of square	*F* Value	*P* Value
Model	9	2367.73	262.96	32.48	<0.0001
A (time)	1	685.91	685.91	84.80	<0.0001
B (enzyme)	1	1319.28	1319.28	163.10	<0.0001
C (temperature)	1	217.15	217.15	26.84	0.0006
A^2 (Time^2)	1	53.99	53.99	6.67	0.0295
B^2 (Enzyme^2)	1	8.04	8.04	0.99	0.3448
C^2 (Temperature^2)	1	8.04	8.04	0.99	0.3448
*A*B*	1	64.63	64.63	7.99	0.0198
*A*C*	1	0.51	0.51	0.06	0.8074
*B*C*	1	0.14	0.14	0.02	0.8962
Residual	9	72.79	8.088		
Lack of fit	5	63.52	12.7043	5.4796	0.0622
Pure error	4	9.27	2.3185		
Cor total	18	2440.52			
R^2	1.00				
Adj R^2	0.99				
CV (%)	4.75				

reduction into α-dextrins.[54] The combined effect of temperature and time was not significant ($p > 0.05$), and the surface shows mainly parallel contour patterns, suggesting additive effects rather than synergistic interaction (Fig. 2b). A similar interaction effect is shown in the hydrolysis of *Ferula assafoetida* protein hydrolysis.[52] Temperature and enzyme concentration also did not exhibit a significant interaction ($p > 0.05$), with hydrolysis efficiency primarily driven by individual factor effects (Fig. 2c). Overall, this indicates that time and enzyme synergy are the main interactive drivers under the tested conditions, while other factor pairs exerted largely independent influences. Similar surface behaviours of temperature, enzyme, and time are observed in the enzymatic hydrolysis of the fish waste.[55]

The accuracy of the quadratic model was confirmed by diagnostic evaluations. The actual *versus* predicted plot showed data points closely aligned along the diagonal, consistent with a high R^2 for hydrolysis efficiency (Fig. 2d), while the residuals *versus* predicted plot exhibited a random scatter around zero (Fig. 2e), indicating no systematic errors or influential outliers. Model optimization using the desirability function in JMP® identified the optimal conditions as a reaction time of 24 h, enzyme dose of 5%, and temperature of 60 °C. Under these conditions, starch hydrolysis efficiency reached 82.8%, closely matching the predicted value of 83.8%, thereby validating the model's reliability. Extrapolation of the fitted RSM polynomial beyond the tested range produced mathematically higher efficiencies (>100%), which are artifacts rather than physically achievable outcomes. To avoid such overestimation, factor ranges were selected to reflect enzyme stability, economic feasibility, and equipment constraints, ensuring that the optimized conditions are both realistic and practically implementable.

Enzymatic hydrolysis of FW has been widely investigated using both single-step and two-step processes, with reported hydrolysis efficiencies and fermentable sugar yields varying considerably depending on feedstock composition, pre-treatment, and enzyme source. Zhang *et al.* reported a high hydrolysis efficiency of 98.5% using a TSEH with α-amylase and glucoamylase, achieving a reducing sugar concentration of 204.2 g L^{-1}, which outperformed acid and alkaline hydrolysis methods.[11] Similarly, Taheri *et al.* achieved 90.3% starch hydrolysis efficiency from fat-extracted FW, yielding 210.1 g L^{-1} fermentable sugars.[56] Salimi *et al.* reported a comparatively lower starch hydrolysis efficiency of 81% using amylolytic enzymes, highlighting the influence of enzyme formulation and process configuration.[57] Hafid *et al.* demonstrated the feasibility of acid-enzyme treatment, achieving an 86.8% hydrolysis efficiency from canteen waste using glucoamylase produced by

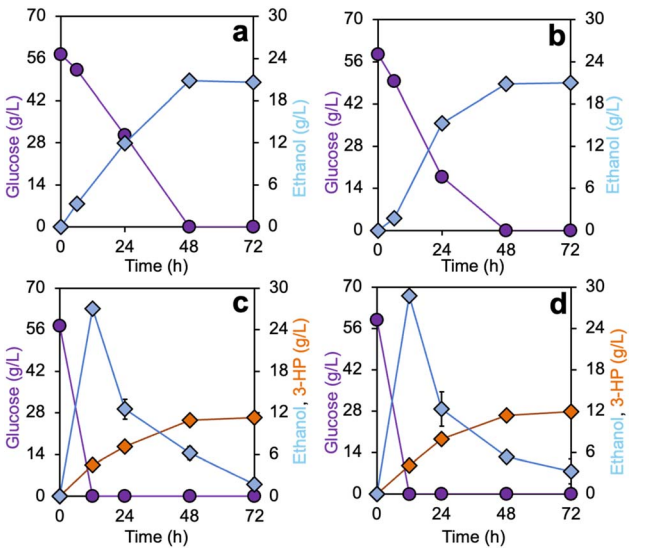

Fig. 3 Time course profile of ethanol fermentation by *S. cerevisiae* from TSEH (a) and OSEH (b) hydrolysates and 3-HP fermentation by *I. orientalis* using TSEH (c) and OSEH (d) hydrolysates. Data represent biological triplicates; error bars indicate the standard deviation (not visible when smaller than the symbol size).

Table 5 Amino acid profile of the proteins obtained from two hydrolysis methods

	Amino acid profile (% crude protein)		
Amino acids %	TSEH	OSEH	Soybean meal[65]
Crude protein	68.23	71.43	46.44
Hydroxyproline	0.12	0.11	—
Aspartic acid	6.36	6.86	—
Threonine	3.21	3.68	4.01
Serine	3.13	3.46	—
Glutamic acid	10.36	10.58	—
Proline	3.87	4.08	—
Glycine	3.05	3.25	—
Alanine	4.05	4.36	—
Cysteine	1.17	1.18	1.42
Valine	4.07	4.49	4.98
Methionine	1.45	1.35	1.35
Isoleucine	3.58	3.63	4.87
Leucine	5.91	6.12	7.79
Tyrosine	2.95	3.29	—
Phenylalanine	3.52	3.72	5.11
Hydroxylysine	1.096	1.029	—
Lysine	4.11	3.89	6.32
Histidine	1.977	1.945	2.54
Arginine	3.484	3.515	7.26
Tryptophan	0.744	0.898	1.44
Σ five key AA[a]	10.69	11.00	14.53

[a] Lysine, methionine, cysteine, threonine, and tryptophan.

Aspergillus niger.[58] Han *et al.* reported a reducing sugar concentration of 39.2 g L^{-1} with a hydrolysis efficiency of 76% when hydrolyzing hamburger waste using commercial α-amylase enzymes, reflecting the impact of feedstock heterogeneity and lower starch content.[59] Overall, these studies underscore the strong dependence of hydrolysis performance on substrate composition, enzyme strategy, and processing configuration, providing a benchmark for evaluating the hydrolysis efficiency and sugar yields obtained in the present study.

3.3 Ethanol and 3-HP fermentation using the glucose hydrolysates

Two hydrolysates from TSEH and OSEH with comparable glucose concentrations of 57.4 and 58.5 g L^{-1} produced a similar ethanol concentration of 20.61 g L^{-1} and 20.96 g L^{-1}, respectively (Fig. 3a and b). Ethanol yields were 70.1% for TSEH and 70.3% for OSEH, corresponding to 0.35 g g^{-1} glucose in both cases. These values are in line with earlier studies on FW substrates, where reported ethanol yields typically range between 0.35–0.44 g g^{-1} glucose, with ethanol titers varying widely (15–87 g L^{-1}) depending on the enzyme cocktails and microorganisms employed.[17,18,60,61] The relatively lower yields could be influenced by inhibitors present in FW hydrolysates. Elevated salt concentrations (indirectly reflected by ash content in Table 1) induced osmotic stress, reducing fermentation rates and extending lag phases.[62] Previous studies showed that >0.5 M salt can lower yeast productivity by ~50%.[63] The final 3-HP concentrations were 11.3 g L^{-1} for TSEH and 12.0 g L^{-1} for OSEH, corresponding to yields of 0.19 g g^{-1} glucose and 0.20 g g^{-1} glucose, respectively (Fig. 3c and d). The strain's tolerance to osmotic stress underscores its suitability for FW hydrolysates.[64] To our knowledge, this is the first study of 3-HP production from kitchen FW hydrolysates, offering a novel strategy for valorising FW into high-value platform chemicals.

3.4 Amino acid profile of protein-rich residues

Enzymatic hydrolysis of D-FW resulted in solid residues that were subsequently lyophilized. The resulting products contained 68.2% proteins from TSEH and 71.4% proteins from OSEH, representing 2.9- and 3-fold increases over R-FW, respectively. Amino acid analysis revealed that both residues possessed

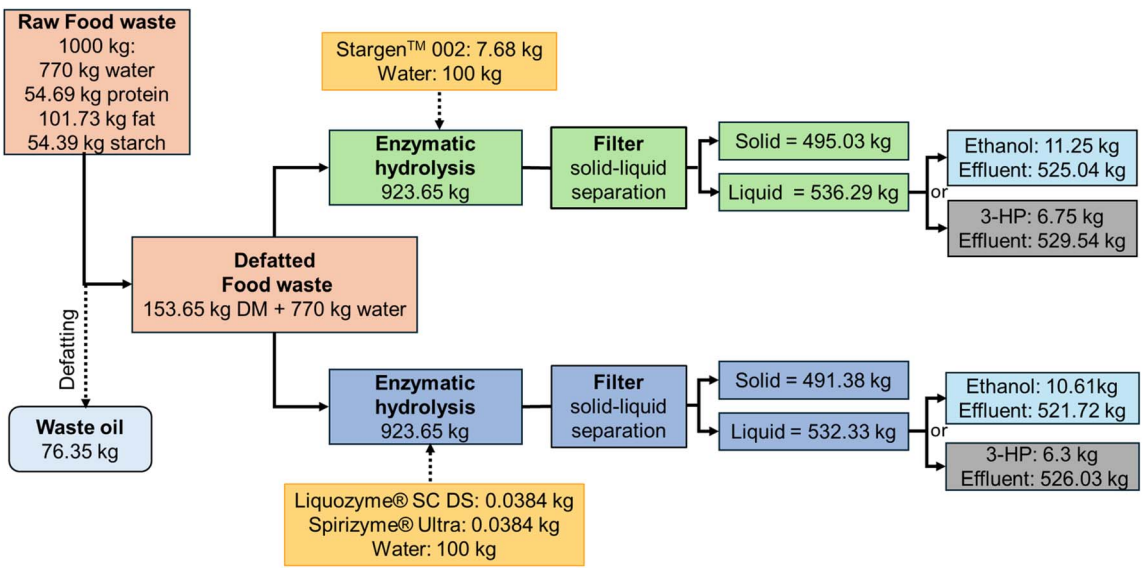

Fig. 4 Mass balance of the FW component-specific conversion strategy.

a broad spectrum of essential and non-essential amino acids (Table 5). Glutamic acid, aspartic acid, leucine, valine, and alanine were the dominant components. In OSEH residues, glutamic acid accounted for 10.6%, followed by aspartic acid (6.9%), leucine (6.1%), and valine (4.5%). TSEH residues exhibited similar patterns with slightly lower values. Trace amounts (<1.1%) of non-proteinogenic amino acids, including taurine, lanthionine, hydroxylysine, and ornithine, were also detected. A comparison with soybean meal from the precision nutrition evaluation database underscores the nutritional significance of these residues, particularly their close match in key amino acids, thereby supporting their potential use in feed formulations.[65]

3.5 Mass balance of the proposed FW valorization pathways

The changes in mass amount of the whole process were calculated based on 1000 Kg of R-FW containing 23% dry matter, ignoring minor mass loss (Fig. 4). From this input, approximately 76.35 kg of FWFs was recovered during the defatting step, which represents a valuable stream for subsequent biodiesel production. The OSEH process yielded 495.03 kg solid residue and 536.29 kg liquid with approximately 60 g L^{-1} glucose concentration. The liquid hydrolysate rich in glucose can be used to produce 11.25 kg of ethanol or 6.75 kg of 3-HP after adding 7.68 kg of Stargen™ 002 and 100 kg of additional water. In contrast, the TSEH process yielded 491.38 kg of solid residue and 532.33 kg of liquid with a similar glucose concentration, which can be used to produce 10.61 kg of ethanol or 6.3 kg of 3-HP after adding 0.07 kg of Liquozyme, Spirizyme, and 100 kg of water. A significant amount of effluent is produced during the ethanol and 3-HP fermentation in both cases. The residual solid fraction, however, might require additional treatment to enhance its suitability for applications such as animal feed.

4. Conclusions

This study demonstrated the feasibility of upgrading kitchen FW through a multi-stream biorefining pathway. Both TSEH and OSHE achieved comparable starch hydrolysis efficiencies (~82%), with OSHE providing a simpler route that yielded 60 g L^{-1} glucose. The resulting glucose hydrolysate was effectively converted into 21 g L^{-1} ethanol or 12 g L^{-1} 3-HP. Additionally, recovered FWFs show potential for biodiesel production, while protein-rich residues may serve as animal feed. Overall, these outcomes highlight that FW can be a versatile feedstock for producing biofuels, platform chemicals, and protein-rich feed ingredients. Such integrated processing enhances resource utilization and supports the transition toward a circular and sustainable bioeconomy.

Conflicts of interest

The authors declare no competing financial interest.

Data availability

The datasets generated during and/or analyzed during the current study are available from the authors on reasonable request.

Acknowledgements

This work is supported by the Agriculture and Food Research Initiative – Foundational and Applied Science Program, project award no. 2024-68016-43831], from the U.S. Department of Agriculture's National Institute of Food and Agriculture. Any opinions, findings, conclusions, or recommendations expressed in this publication are those of the author(s) and should not be construed to represent any official USDA or U.S. Government determination or policy.

References

1 Food loss and food waste, Food and Agriculture Organization of the United Nations, Rome Italy, https://www.fao.org/4/mb060e/mb060e.pdf, (accessed 15 March 2025).
2 S. Arvelli, L. Jia, M. Zhang and J. Zhao, *J. Agric. Food Chem.*, 2025, **73**, 16085–16108.
3 N. Rai, T. L. Pavankumar, B. Ghotra, S. Dhillon, V. Juneja, N. Amaly and P. Pandey, *Front. Sustain. Food Syst.*, 2025, **9**, 1575113.
4 P. Brancoli, K. Bolton and M. Eriksson, *Waste Manage.*, 2020, **117**, 136–145.
5 H. S. Kusuma, A. Sabita, N. A. Putri, N. Azliza, N. Illiyanasafa, H. Darmokoesoemo, A. N. Amenaghawon and T. A. Kurniawan, *Food Chem.:Mol. Sci.*, 2024, **9**, 100225.
6 H. M. Abdel-Mageed, A. Z. Barakat, R. I. Bassuiny, A. M. Elsayed, H. A. Salah, A. M. Abdel-Aty and S. A. Mohamed, *Folia Microbiol.*, 2022, **67**, 253–264.
7 M. A. Frezzini, L. Massimi, M. L. Astolfi, S. Canepari and A. Giuliano, *Materials*, 2019, **12**, 4242.
8 T. H. Kwan, Y. Hu and C. S. K. Lin, *J. Cleaner Prod.*, 2018, **181**, 72–87.
9 B. J. E. de, M. M. Annevelink, Task 42 Biorefining in a Circular Economy, 2021.
10 D. A. Teigiserova, L. Hamelin and M. Thomsen, *Sci. Total Environ.*, 2020, **706**, 136033.
11 C. Zhang, X. Kang, F. Wang, Y. Tian, T. Liu, Y. Su, T. Qian and Y. Zhang, *Energy*, 2020, **208**, 118379.
12 V. Narisetty, N. Adlakha, N. Kumar Singh, S. K. Dalei, A. A. Prabhu, S. Nagarajan, A. Naresh Kumar, J. Amruthraj Nagoth, G. Kumar, V. Singh and V. Kumar, *Bioresour. Technol.*, 2022, **363**, 127856.
13 E. Palmqvist and B. Hahn-Hägerdal, *Bioresour. Technol.*, 2000, **74**, 25–33.
14 N. A. Sagar, M. Pathak, H. Sati, S. Agarwal and S. Pareek, *Trends Food Sci. Technol.*, 2024, **147**, 104413.
15 Y. Lv, Y. Zhang and Y. Xu, *Biomass Bioenergy*, 2024, **183**, 107133.
16 C. E. R. Reis, N. Libardi Junior, H. B. S. Bento, A. K. F. de Carvalho, L. P. de S. Vandenberghe, C. R. Soccol, T. M. Aminabhavi and A. K. Chandel, *Chem. Eng. J.*, 2023, **451**, 138690.
17 G. Prasoulas, A. Gentikis, A. Konti, S. Kalantzi, D. Kekos and D. Mamma, *Fermentation*, 2020, **6**, 39.

18 I. Ntaikou, G. Antonopoulou and G. Lyberatos, *Sustainability*, 2020, **13**, 259.
19 A. Anand, K. Kumar, K. C. Khaire, K. Roy and V. S. Moholkar, *Bioresour. Technol. Rep.*, 2024, **27**, 101932.
20 I. Caro, C. Marzo-Gago, A. B. Díaz and A. Blandino, *J. Environ. Chem. Eng.*, 2024, **12**, 111862.
21 T. P. G. A. A. B. J. H. J. W. J. M. A. E. D. L. L. and J. S. Werpy, Top Value Added Chemicals from Biomass. Volume 1-Results of Screening for Potential Candidates from Sugars and Synthesis Gas, Department of Energy, Washington, DC, USA, 2004.
22 S. Lertsriwong, P. Khaosaart, N. Boonvitthya, W. Chulalaksananukul and C. Glinwong, *Synth. Syst. Biotechnol.*, 2025, **10**, 1077–1086.
23 M. Bourgeois, S. Taussac, N. Bernet, R. Escudié and E. Trably, *Environ. Technol. Innovation*, 2025, **39**, 104324.
24 H. Peng, M. Li, K. Wang, K. K. Sahoo, D. Jeong, L. Jia, S. Pandey, E. J. Oh, J. Dong, J. Lee, J. Qi, N. Arabi, S. Babaei, S. Arvelli, S.-T. Yang, M. Zhang and J. Zhao, *Green Chem.*, 2025, **27**, 13682–13691.
25 S. I. Pirani and H. A. Arafat, *J. Cleaner Prod.*, 2016, **132**, 129–145.
26 R. Z. K. Hussein, N. K. Attia, M. K. Fouad and S. T. ElSheltawy, *Biomass Bioenergy*, 2021, **144**, 105850.
27 Y. Zhao, K. Zhu, J. Li, Y. Zhao, S. Li, C. Zhang, D. Xiao and A. Yu, *Microb. Biotechnol.*, 2021, **14**, 2497–2513.
28 G. Djohan and M. Ibadurrohman, *Slamet*, 2019, 020075.
29 D. Liu, Y. Shen, P. T. Wai, H. Agus, P. Zhang, P. Jiang, Z. Nie, G. Jiang, H. Zhao and M. Zhao, *J. Appl. Polym. Sci.*, 2021, **138**, 50128.
30 S. Pan, J. Yan, X. Peng, Z. Xu, Q. Zeng, Z. Wang, M. Zhao and Y. Chen, *ACS Sustain. Chem. Eng.*, 2023, **11**, 1492–1501.
31 M. Cappello, S. Filippi, D. Rossi, P. Cinelli, I. Anguillesi, C. Camodeca, E. Orlandini, G. Polacco and M. Seggiani, *Sustainability*, 2024, **16**, 9456.
32 K. Polaczek, M. Kurańska and A. Prociak, *J. Cleaner Prod.*, 2022, **359**, 132107.
33 K. Sharma, S. S. Toor, J. Brandão, T. H. Pedersen and L. A. Rosendahl, *J. Cleaner Prod.*, 2021, **294**, 126214.
34 Y. Hou, Z. Wu, Z. Dai, G. Wang and G. Wu, *J. Anim. Sci. Biotechnol.*, 2017, **8**, 24.
35 P. Bohutskyi, K. Liu, B. A. Kessler, T. Kula, Y. Hong, E. J. Bouwer, M. J. Betenbaugh and F. C. T. Allnutt, *Appl. Microbiol. Biotechnol.*, 2014, **98**, 5261–5273.
36 T. Schmidt, M. Nelles, F. Scholwin and J. Pröter, *Bioresour. Technol.*, 2014, **168**, 80–85.
37 H. M. Oliveira, A. Q. Pinheiro, A. J. M. Fonseca, A. R. J. Cabrita and M. R. G. Maia, *Ultrason. Sonochem.*, 2018, **49**, 128–136.
38 Y. Xu and D. Wang, *Appl. Energy*, 2017, **195**, 196–203.
39 D. Jeong, D. Lee, J. Liu, S. R. Kim, Y.-S. Jin, J. Zhao and E. J. Oh, *Bioresour. Technol.*, 2025, **437**, 133113.
40 S. Arvelli, M. Liu, G. Chen, T. Weiss, Y. Zhang, Y. Li, D. Wang and Y. Zheng, *LWT–Food Sci. Technol.*, 2024, **203**, 116407.
41 X. Kong, Y. Wei, S. Xu, J. Liu, H. Li, Y. Liu and S. Yu, *Bioresour. Technol.*, 2016, **211**, 65–71.
42 A. Patel, I. Delgado Vellosillo, U. Rova, L. Matsakas and P. Christakopoulos, *Chem. Eng. J.*, 2022, **431**, 133955.
43 M. Khammassi, G. Amato, L. Caputo, F. Nazzaro, F. Fratianni, H. Kouki, I. Amri, L. Hamrouni and V. De Feo, *Molecules*, 2023, **29**, 160.
44 H. Teng and L. Chen, *Crit. Rev. Food Sci. Nutr.*, 2017, **57**, 3438–3448.
45 K. He, Y. Liu, L. Tian, W. He and Q. Cheng, *Heliyon*, 2024, **10**, e28200.
46 T.-K. Kim, J.-H. Lee, H. I. Yong, M.-C. Kang, J. Y. Cha, J. Y. Chun and Y.-S. Choi, *Foods*, 2022, **11**, 1400.
47 G. Pellerin and A. Doyen, *Food Chem.*, 2024, **448**, 139149.
48 D. Singh, D. Sharma, S. L. Soni, S. Sharma and D. Kumari, *Fuel*, 2019, **253**, 60–71.
49 J. Orsavova, L. Misurcova, J. Ambrozova, R. Vicha and J. Mlcek, *Int. J. Mol. Sci.*, 2015, **16**, 12871–12890.
50 R. L. McCormick, G. M. Fioroni, S. Y. Mohamed, N. Naser, T. L. Alleman, S. Kim, Z. Wang, Y. Lin, Y. Ju and K. Kar, *Fuel Commun.*, 2024, **19**, 100120.
51 R. D. Lanjekar and D. Deshmukh, *Renewable Sustainable Energy Rev.*, 2016, **54**, 1401–1411.
52 A. A. Gholami, M. S. Taghizadeh, A. Afsharifar, A. Moghadam, Z.-S. Mortazavi and A. Niazi, *Appl. Food Res.*, 2025, **5**, 100915.
53 C. Aenglong, W. Woonnoi, S. Tanasawet, W. Klaypradit and W. Sukketsiri, *Rice*, 2024, **17**, 13.
54 R. Benítez Benítez, W. F. Elvira Tabares, L. A. Lenis Velásquez, C. I. Hurtado Sánchez and O. A. Salinas Cruel, *Heliyon*, 2021, **7**, e07817.
55 K. Korkmaz and B. Tokur, *Food Biosci.*, 2022, **45**, 101312.
56 M. E. Taheri, E. Salimi, K. Saragas, J. Novakovic, E. M. Barampouti, S. Mai, D. Malamis, K. Moustakas and M. Loizidou, *Biomass Convers. Biorefin.*, 2021, **11**, 219–226.
57 E. Salimi, K. Saragas, M. E. Taheri, J. Novakovic, E. M. Barampouti, S. Mai, K. Moustakas, D. Malamis and M. Loizidou, *Waste Biomass Valorization*, 2019, **10**, 3753–3762.
58 H. S. Hafid, A. R. Nor 'Aini, M. N. Mokhtar, A. T. Talib, A. S. Baharuddin and M. S. Umi Kalsom, *Waste Manage.*, 2017, **67**, 95–105.
59 W. Han, Y. Liu, X. Xu, J. Huang, H. He, L. Chen, S. Qiu, J. Tang and P. Hou, *J. Cleaner Prod.*, 2020, **264**, 121658.
60 Z. Ling, S. Wang, Z. Leng, C. Li, W. Zhang, X. Kang, X. Qi and C. Zhang, *Energy Fuels*, 2023, **37**, 14936–14945.
61 F. Chatzimaliakas, D. Christianides, D. Malamis, S. Mai and E. M. Barampouti, *Sustainability*, 2023, **15**, 16349.
62 M. Postaru, A. Tucaliuc, D. Cascaval and A.-I. Galaction, *Microorganisms*, 2023, **11**, 2522.
63 E. Casey, N. S. Mosier, J. Adamec, Z. Stockdale, N. Ho and M. Sedlak, *Biotechnol. Biofuels*, 2013, **6**, 83.
64 S.-I. Tan, Z. Liu, V. G. Tran, T. A. Martin and H. Zhao, *Metab. Eng.*, 2025, **89**, 12–21.
65 E. O. Oviedo-Rondón, A. Toscan, N. S. Fagundes, J. K. Vidal, J. Barbi and P. Thiery, *J. Appl. Poult. Res.*, 2024, **33**, 100448.